Original Paper

Cellular Physiology and Biochemistry

Cell Physiol Biochem 2011;27:443-452

Accepted: March 30, 2011

Structural Basis of Slow Activation Gating in the Cardiac I_{Ks} Channel Complex

Nathalie Strutz-Seebohm[1], Michael Pusch[2], Steffen Wolf[3,4], Raphael Stoll[5], Daniel Tapken[6], Klaus Gerwert[3,4], Bernard Attali[7] and Guiscard Seebohm[1]

[1]Department of Biochemistry I - Cation Channel Group, Ruhr University, Bochum, [2]Istituto di Biofisica, Genova, [3]Department of Biophysics, CAS–Max-Planck Partner Institute for Computational Biology (PICB), Shanghai Institutes for Biological Sciences (SIBS), Shanghai, [4]Department of Biophysics, Ruhr University, Bochum, [5]Department of Biochemistry II - Biomolecular NMR Spectroscopy Group, Ruhr University, Bochum, [6]Department of Medicinal Chemistry - Biostructural Research Group, Faculty of Pharmaceutical Sciences, University of Copenhagen, Copenhagen, [7]Department of Physiology and Pharmacology, Sackler Faculty of Medicine, Tel Aviv University, Ramat Aviv

Key Words
KCNQ1/KCNE1 • Structure • Model

Abstract
Accessory β-subunits of the KCNE gene family modulate the function of various cation channel α-subunits by the formation of heteromultimers. Among the most dramatic changes of biophysical properties of a voltage-gated channel by KCNEs are the effects of KCNE1 on KCNQ1 channels. KCNQ1 and KCNE1 are believed to form native I_{Ks} channels. Here, we characterize molecular determinants of KCNE1 interaction with KCNQ1 channels by scanning mutagenesis, double mutant cycle analysis, and molecular dynamics simulations. Our findings suggest that KCNE1 binds to the outer face of the KCNQ1 channel pore domain, modifies interactions between voltage sensor, S4-S5 linker and the pore domain, leading to structural modifications of the selectivity filter and voltage sensor domain. Molecular dynamics simulations suggest a stable interaction of the KCNE1 transmembrane α-helix with the pore domain S5/S6 and part of the voltage sensor domain S4 of KCNQ1 in a putative pre-open channel state. Formation of this state may induce slow activation gating, the pivotal characteristic of native cardiac I_{Ks} channels. This new KCNQ1-KCNE1 model may become useful for dynamic modeling of disease-associated mutant I_{Ks} channels.

Introduction

KCNE accessory subunits modify the biophysical properties of several voltage-gated cation channels in ways that often recapitulate the characteristics of native currents in various tissues. A broad variety of channels may recruit KCNE β-subunits, including KCNQ1[1, 2], ERG [3], HCN4 [4], Kv1.1, Kv1.3 [5], Kv2.1, Kv3.1 [6], and Kv4.3 [7, 8]. Modulation of voltage-gated KCNQ1 channels by KCNE1 (MinK, IsK) causes the most dramatic change in biophysical properties. Homotetrameric KCNQ1 (KvLQT1, Kv7.1) channels activate with relatively fast kinetics and partially inactivate. In contrast, KCNQ1/KCNE1 heteromeric channels activate far more slowly at more positive potentials, do not inactivate and have an increased single channel conductance [1, 2, 9, 10]. KCNQ1/KCNE1 channel current resembles the cardiac slow delayed rectifier

KARGER
Fax +41 61 306 12 34
E-Mail karger@karger.ch
www.karger.com

1015-8987/11/0275-0443$38.00/0

Accessible online at:
www.karger.com/cpb

G. Seebohm
Department of Biochemistry I - Cation Channel Group
Ruhr University Bochum (Germany)
Tel. +49 234 32-24233, Fax +49 234 32-14034
E-Mail guiscard.seebohm@rub.de

potassium current I_{Ks}, which contributes to terminal repolarization of the cardiac action potential. Mutations in *KCNE1* or *KCNQ1* reduce I_{Ks} and cause long QT syndrome (LQTS), predisposing affected individuals to arrhythmia and sudden cardiac death [1, 2]. Disease-associated mutations in KCNQ1 or KCNE1 might directly, or through an allosteric mechanism, prevent interactions of KCNE1 with its binding region on the channel [11]. The stoichiometry of KCNQ1/KCNE1 channels was reported to be variable [12, 13], or a fixed stoichiometry of 4 KCNQ1 α-subunits to 2 KCNE1 β-subunits in functional channel complexes was suggested [14, 15]. A direct interaction of the transmembrane domains of KCNQ1 with KCNE1 has been proposed, but the specific amino acid interactions remains controversial [16-23]. The solution NMR structure of a synthetic partial KCNE1 peptide (K27: KLEALYILMVLGFFGFFTLGIMLSYI) shows that this peptide adopts an α-helical structure [24]. Recently, the NMR structures of full-length KCNE1 confirmed that the transmembrane domain of KCNE1 is an α-helix that is flexible around the central T58. A model based on NMR-structural coordinates and Rosetta-dockings of KCNE1 to KCNQ1 suggest binding of KCNE1 to a "gain-of-function cleft" [25].

Here, we study the interaction of KCNE1 with KCNQ1 in the closed state using double mutant cycle analysis. We incorporate our experimental results into a 3D model and perform Molecular Dynamics (MD) simulations to assess the stability of the modeled channel complex as well as to analyze further molecular details. Our model may represent a pre-open closed state and is in good agreement with recent results of several experimental studies [12-15, 21-23]. The modeled structure suggests a molecular basis for the slow activation of I_{Ks}.

Materials and Methods

Oocyte expression

Xenopus laevis frogs were anesthetized with tricaine (0.17%) and ovarian lobes were removed. The ovarian lobes were cut into small pieces and enzymatically treated for 1.5-2 h with collagenase (1 mg/ml, Worthington, type II) at room temperature in Ca^{2+}-free ND96 solution, containing in mM: 96 NaCl, 2 KCl, 1 $MgCl_2$, 5 HEPES (pH 7.6). Stage V oocytes were collected and injected with 50 nl of RNA. Oocytes were injected with 1 ng *Kv1.5* cRNA, 5 ng of *KCNQ1* cRNA, or 5 ng *KCNQ1* cRNA plus 1 ng of *KCNE1* cRNA. Oocytes were maintained at 17-18 C in ND96 storage solution (in mM: 96 NaCl, 4 KCl, 1.8 $MgCl_2$, 0.1 $CaCl_2$, 5 HEPES (4-(2-hydroxyethyl)-1-piperazineethanesulfonic acid), gentamicin (50 mg/l); pH 7.6).

Electrophysiology

Whole-cell currents in *Xenopus* oocytes were recorded with standard two-electrode voltage clamp techniques with a Turbo TEC10-CX amplifier (npi) at room temperature (22-24 C). Data were acquired with Clampex (pCLAMP 8.0, Axon Instruments) and analyzed with Clampfit (pCLAMP 8.0, Axon Instruments), the custom program Ana, and Origin 6.0 (Microcal). Whole cell currents were recorded in ND96 recording solution (in mM: 96 NaCl, 4 KCl, 1.8 $MgCl_2$, 0.1 $CaCl_2$, 5 HEPES; pH 7.6).

Molecular biology

Site-directed mutagenesis of *KCNQ1* cDNA subcloned into the pSGEM vector was performed by PCR using the megaprimer method and Pfu polymerase. All constructs were confirmed by automated DNA sequencing. *KCNE1* cDNA was subcloned into the pSP64 vector. The constructs were linearized with NheI or EcoRI. *In vitro* synthesis of poly-A-capped cRNA was performed with SP6 and T7 mMessage mMachine kits (Ambion).

Molecular modeling and MD simulations

A consensus KCNQ1 homology model was generated using YASARA (YASARA Biosciences, Vienna, Austria). Ten different KCNE1 models with different bending at central glycines (G52, G55 and G60) were generated. Docking of energy-optimized KCNE1 conformers to the KCNQ1 S5-S6 homology model was performed using an α-helix packing approach with the Global Range Molecular Matching program (GRAMM v1.03 [26]). The non-covalent bond finder 9 was used to further determine the interaction of the favoured KCNE1 molecule with its putative binding site in KCNQ1. The model that positioned T58 and S338 in close proximity was chosen for molecular dynamics simulations. Molecular dynamics all atoms mobile. The model was placed in an explicit membrane/solvent environment. Free MD simulations were performed with GROMACS [27] based on a protocol for the simulation of membrane protein homology models. Model building and MD simulation settings are described in more detail in the supplementary material section (http://www.ruhr-uni-bochum.de/bc1/kation/download/Strutz-Seebohm_et_al_Cell_Physiol_Biochem_supplementary_material.doc).

Double-mutant cycle analysis

The steady state activation curve was obtained by tail current analysis from pulse protocols employing a fixed "tail" pulse to 0 mV [28].

The resulting curve was fitted by

$$I_{tail}(V) = \frac{I_{max}}{1 + e^{-\frac{\Delta G_0 + zV}{RT}}}$$

where I_{max} is the (estimated) maximal current, z the apparent gating valence, R the universal gas constant, T the absolute temperature, and ΔG_0 the free energy difference between the closed and the open state at zero voltage. This description is based on the simplifying assumption that gating can be described by a two-state process. The resulting values for ΔG_0 were averaged. ΔG_0 values are expressed in units of RT (see

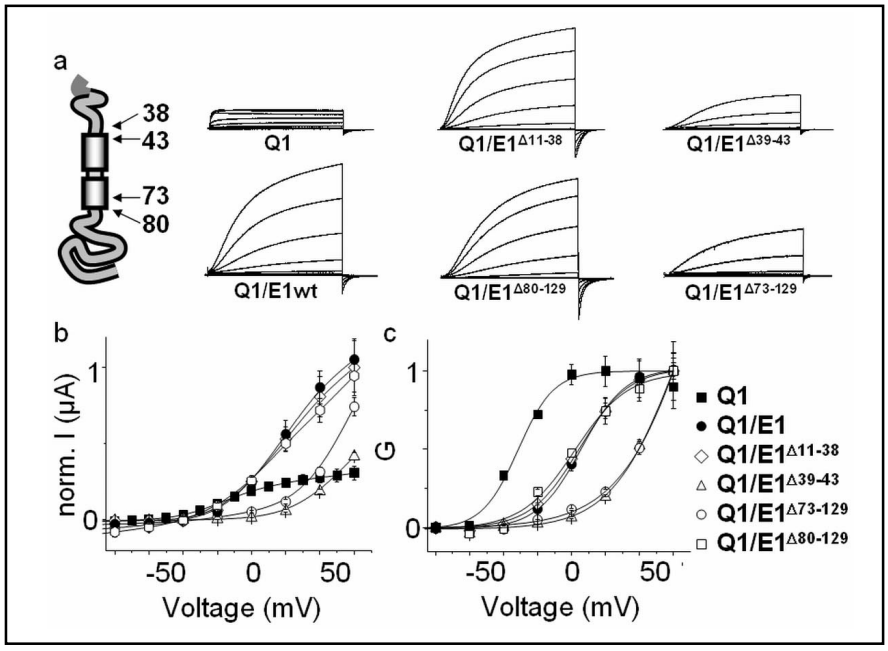

Fig. 1. Secondary structure of KCNE1 and identification of regions important for specific effects of KCNE1 on KCNQ1. a, The cartoon on the left shows the secondary structure of KCNE1 and the positions of the borders of segments that were deleted to identify regions in KCNE1 important for effects on KCNQ1. Representative current traces of KCNQ1 (Q1) expressed in the absence or presence of KCNE1 (E1) wild type or the four different deletion mutants are shown. The pulse protocol used is indicated above. b, Current amplitudes were analyzed and plotted vs. potentials. c, GV curves were determined by tail current analysis.

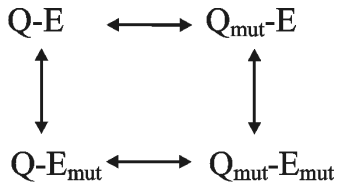

Fig. 2). The voltage of half-maximal activation ($V_{1/2}$) is related to ΔG_0 by $V_{1/2} = -\Delta G_0/z$. The following state model was used to calculate putative interaction energies.

The state Q-E denotes the heteromeric KCNQ1/KCNE1 channel, Q_{mut}-E denotes the heteromeric KCNQ1(mutated)/KCNE1(wt) channel, etc. The coupling energy, $\Delta\Delta G$, reported in Fig. 2, was calculated by

$\Delta\Delta G = [\Delta G_0(Q_{Mut}\text{-}E_{Mut}) - \Delta G_0(Q\text{-}E_{Mut})] - [\Delta G_0(Q_{Mut}\text{-}E) - \Delta G_0(Q\text{-}E)]$

Results and Discussion

The structural basis of KCNE1 subunit interaction with the KCNQ1 channel was previously explored by determining the functional effects of deletion of the N- or C-termini of KCNE1 [29]. Here, we show that deletion of residues 11-38 (Δ11-38) or truncation of 49 amino acids from the C-terminus (Δ80-129) do not impair the ability of KCNE1 to slow the rate or shift the voltage dependence of KCNQ1 channel activation. However, deletion of amino acids 39-43 (Δ39-43) or truncation of 56 amino acids from the C-terminus (Δ73-129) caused a further rightward shift in the voltage dependence of activation resulting in smaller currents at 60 mV (Fig. 1).

Alanine scan and double-mutant cycle analysis identify putative interaction sites between KCNE1 and KCNQ1

To identify putative sites of interaction between KCNE1 and the KCNQ1 channel, we employed a scanning mutagenesis approach, introducing point mutations into the S5 and S6 domains of the KCNQ1 α-subunit. Residues were individually mutated to alanines. If the wild type sequence contained an alanine, it was mutated to cysteine [29]. These mutants or the KCNQ1 wild type were expressed in *Xenopus* oocytes in the absence or presence of KCNE1. Coexpression of KCNE1 resulted in a shift in the $V_{1/2}$ of the wild-type KCNQ1 activation curve by +45 mV. Individual alanine substitutions of five residues in S5 and three residues in S6 of KCNQ1 reduced this shift by KCNE1. The four mutations Y267A, F270A, F339A, and F340A had the most pronounced effects, reducing the shift of the $V_{1/2}$ of activation to values of less than +23 mV, while L271A, I274A, F275A, and A344C mutations caused only a minor reduction (Fig. 2A).

To gain further insight into the interactions of these residues in KCNQ1 with KCNE1, we used double-mutant cycle analysis, a method allowing to measure the strength of intramolecular and intermolecular interactions in proteins [30]. It involves analysis of the free energy of transition between two states – in this study the open and closed channel state – for a wild-type protein, two single mutants, and the corresponding double mutant. From these free energies, the free energy changes caused by the mutations can be calculated. If the two mutated residues

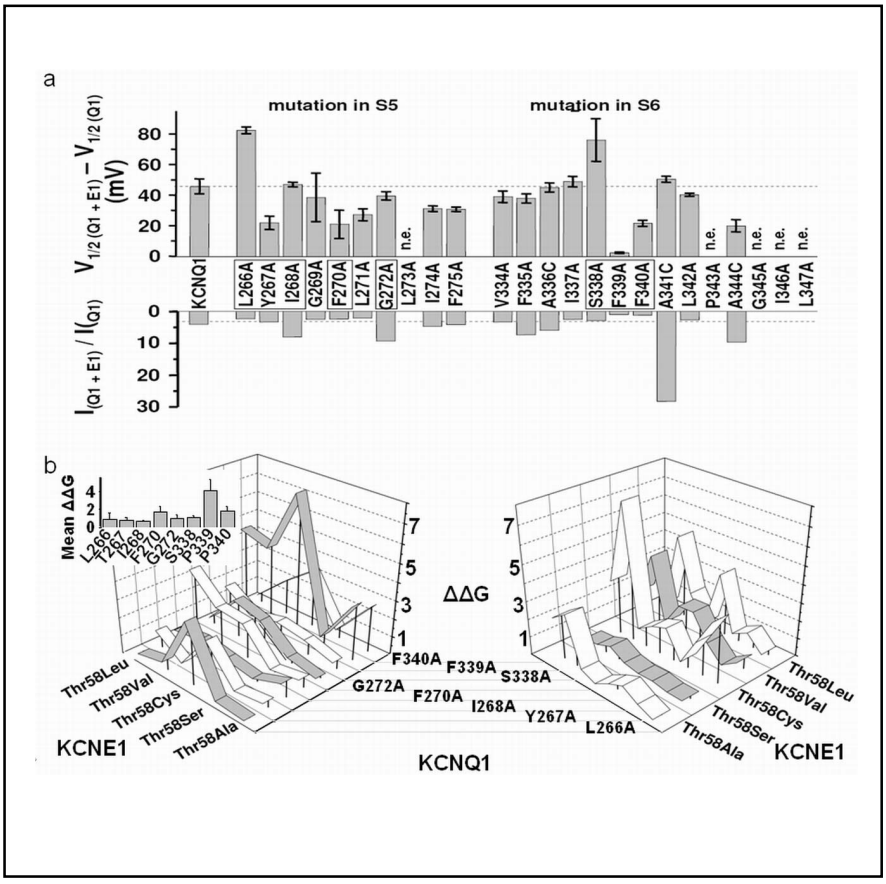

Fig. 2. Alanine scan and double-mutant cycle analysis of S5 and S6 to identify putative interaction sites between KCNQ1 and KCNE1. a, Several amino acids in S5 and S6 of KCNQ1 were individually mutated to alanines (native Ala to Cys), and the channels were recorded in the absence or presence of KCNE1. The respective GV curves were determined by tail current analysis, and the effects of KCNE1 coexpression on GV were expressed as the differences in the voltages of half-maximal activation $V_{1/2(Q1+E1)} - V_{1/2(Q1)}$. Effects of KCNE1 coexpression on amplitudes of currents recorded at 40 mV are presented as I_{Q1+E1}/I_{Q1} (n = 8–24). b, Double-mutant cycle analysis of selected KCNQ1 mutants with 5 KCNE1 T58X mutants. The ΔΔG values were calculated from GV curves obtained from tail currents (n = 6–14) as described in Methods. The ΔΔG values (in units of RT) are plotted vs. the respective KCNE1 and KCNQ1 mutant (left) or plotted vs. the respective KCNE1 mutant to show the mild energetic perturbances by mutation T58S (right). The mean ΔΔG effects by the respective KCNQ1 mutant are shown in the small upper left inlay.

interact either directly or indirectly, the free energy change for the double mutation differs from the sum of the energy changes for the single mutations, and a coupling energy *ΔΔG* between the two residues can be calculated (Fig. 2). Using this method, we explored the interactions of the four key residues in KCNQ1 described above as well as of four additional residues located in close proximity to these key residues with the residue T58 of KCNE1. This residue was previously reported to be crucial for KCNE subtype-selective effects on KCNQ1 [12, 31]. For this analysis, we coexpressed KCNQ1 wild type and the eight mutant subunits with KCNE1 wild type and five different mutants containing mutations of T58 to either A, S, C, V, or L. We found the strongest energetic coupling of T58 in KCNE1 with F339 in KCNQ1 (mean $\Delta\Delta G$=1.5–4.5 *RT*), followed by F340 and F270, suggesting a possible direct interaction of F339 in KCNQ1 with T58 in KCNE1 (Fig. 2b). The results further show a weak dependence of energetic coupling on the volume of residue 58 in KCNE1: Compared to substitutions with a small side chain, substitution of T58 with larger residues or a Ser with hydrogen bonding capabilities resulted in a shift of the voltage dependence of activation to more positive potentials (Fig. 2b). A good candidate for hydrogen bond formation with T58 is the KCNQ1 residue S338. However, mutation of S338 to alanine shifted the voltage dependence of activation by +70 mV independent of the specific mutation of T58. F270A, F339A and F340A mutations impaired both the putative hydrogen bonding effects and the volume effects. This may be the result of F339A and F340A positioning S338 to allow for the putative hydrogen bonding. Although double-mutant cycle analysis cannot easily distinguish between direct and allosteric protein-protein interactions, these data suggest that KCNE1 binds to specific residues of the S5 and S6 domains of KCNQ1. Combined with previous results obtained by analysis of mutations in S4 [23], our findings suggest that KCNE1 is positioned between S4 and S5/S6 of KCNQ1.

The putative KCNQ1-KCNE1 interactions defined by mutation analyses were corroborated by molecular modeling. We utilized a homology model of the S1-S6 domains of KCNQ1 based on the Kv1.2 K^+ channel crystal structure [32-34]. The KCNE1 transmembrane domain was constructed as an α-helix in agreement with previous reports [24, 25, 31]. We docked several conformers of this putative KCNE1 transmembrane peptide to the tetrameric KCNQ1 channel open state homology model, allowing flexibility at glycines in the

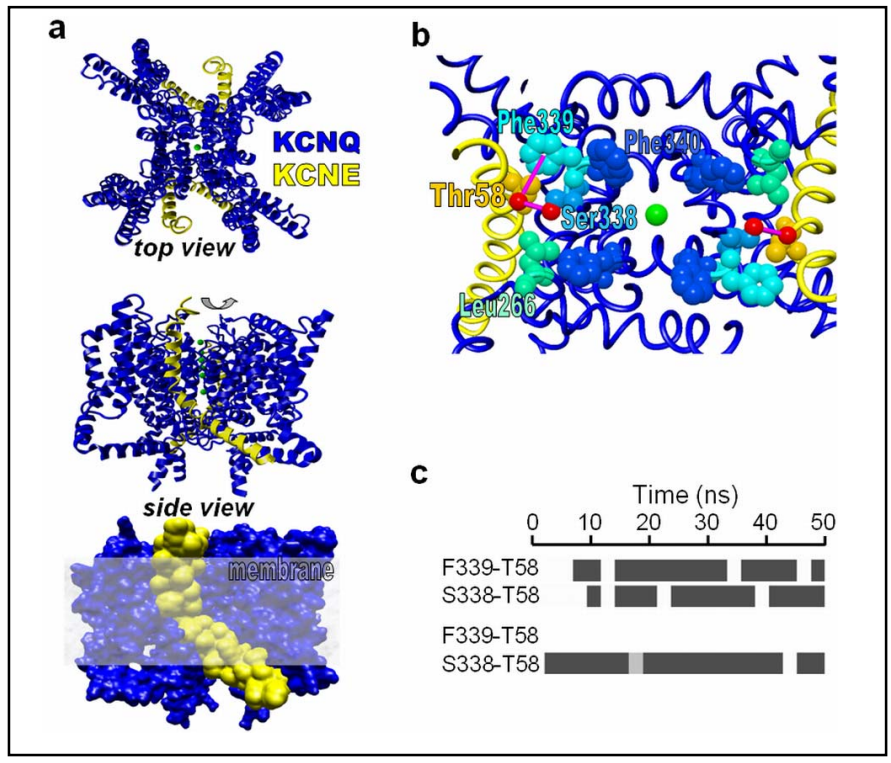

Fig. 3. 3D homology model of the KCNQ1/KCNE1 channel. a, 3D model of the KCNQ1/KCNE1 channel complex. KCNQ1 (amino acids 89-358) was modeled based on homology to known Kv1.2 channel structures (see methods). The KCNE1 model (amino acids 39-79) was *de novo* created as a straight α-helix. Two KCNE1 molecules were docked to KCNQ1, positioning T58 of KCNE1 in close proximity to F339 of KCNQ1 with assumed flexibility at three central glycines. The KCNQ1/KCNE1 model is shown in top and side views. The position of the membrane is shown in the space filling model below. b, Functionally important residues (KCNQ1: L266, S338, F339, and F340; KCNE1: T58) are positioned in a plane. Residues KCNQ1-S338 and KCNE1-T58 are positioned in close proximity to possibly favor hydrogen bonding (pink line). c, The S338/T58 hydrogen bond (gray bars) in MD simulations. The global complex converged to a stable structure during the last 10 ns of this simulation. The the putative hydrogen-bonding oxygen atoms of KCNQ1-S338 and KCNE1-T58 as well as KCNQ1-F339 (π-system) and KCNE1-T58 were analyzed for distances and geometries characteristic of hydrogen bonds. The analyses show that whereas one putative hydrogen bond system is present only in one subunit (putative hydrogen bond distance/geometry between KCNQ1-F339 (π-system) and KCNE1-T58: 71%/0%), the other one is relatively stable in both subunits during the simulation (putative hydrogen bond distance/geometry between KCNQ1-S338 and KCNE1-T58: 66%/85%). (The pdb-file can be downloaded from our web-page under: http://www.ruhr-uni-bochum.de/bc1/kation/download/Q1E1-nach_50_ns_sim_average_a.pdb).

center of the KCNE1 peptide as suggested by a previous NMR study [25]. For further analysis we chose the model that positioned the amino acid T58 in close proximity to F270, S338, F339, and F340, in accordance with the results from our double-mutant cycle analysis. Under these constraints a kinking of KCNE1 and a kinking of the S4-S5 linker in KCNQ1 with subsequent S4 repositioning were required in order to allow direct interactions of T58 in KCNE1 and closest proximity of F270 and F340 in KCNQ1 with the KCNQ1 residues S338 and F339. In the final energy-optimized model the central KCNE1 helix resides in a position between S4, S5, and S6, with its C-terminal part kinked towards the adjacent subunit. This model differs in several details from previous models that model the KCNE1 transmembrane domain as a straight helix and position it to the crevice between the pore domain S1-S4 and the pore domain S5-S6 as well [20, 23, 35].

Two KCNE1 peptides were docked to a tetrameric KCNQ1 channel model to satisfy experimental data suggesting the stoichiometry of 4 α-subunits with 2 β-subunits and still satisfy the model of a variable stoichiometry as suggested by others as this stoichiometry is one possible stoichiometry in a variable model [12-15].

In order to analyze whether this 3D model represents a stable channel complex we applied molecular dynamics. We incorporated the model in an explicit solvent/membrane model and conducted free MD simulations of 50 ns simulated time. Over the first 40 ns the voltage sensors tended to tilt slightly and remained stable for the last 10 ns of the simulation. Apart from these movements, the model remained intact during simulation of 50 ns, and the relatively small RMSD values of the transmembrane α-helices indicate a stable conformation of this channel complex.

Our model is in good agreement with the experimental data presented herein, as it explains the effects of mutations at the following residues:

- KCNQ1 residue F339 directly interacts with KCNE1 residue T58. The side chain of F339 interacts with the Cγ or the hydroxyl group of T58 (Fig. 3b,c).

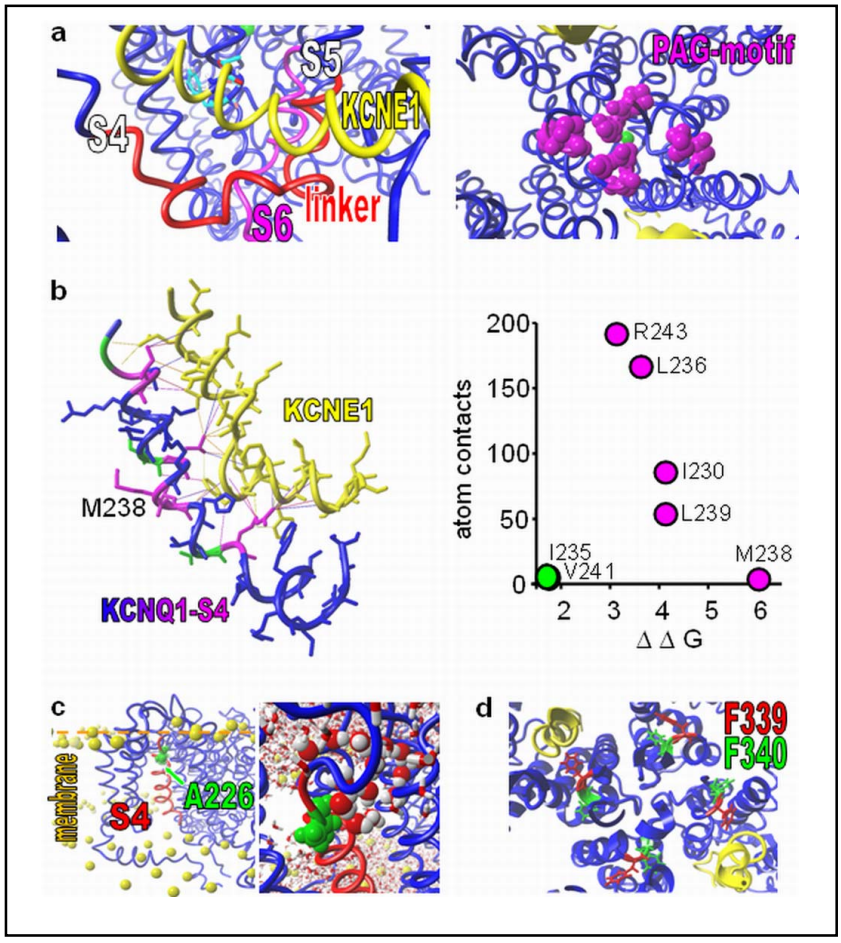

Fig. 4. Comparison of the 3D model of the KCNQ1/KCNE1 channel with published data. a, A close view on the S4-linker-S5 region (red), KCNE1 (yellow) and the lower S6 (magenta). The key residues KCNQ1-S338, KCNQ1-F339 and KCNE1-T58 are colored according to the CPK color code. After the 50 ns simulation the S4-linker-S5 region and the lower S6 of the adjacent subunit are denatured, whereas KCNE1 retains its α-helical fold. These effects by KCNE1 lead to a closing of the bundle crossing (right). The PAG motif of two adjacent KCNQ1 subunits close the pore, whereas the other two KCNQ1 subunits stay in an open position. b, The S4 helix of KCNQ1 (residues 229–244) and KCNE1 (residues 39–63) are shown in stick representation. KCNE1 residues are colored yellow. KCNQ1 residues that were reported to be energetically linked to KCNE1 are colored green and magenta [23]. KCNQ1 residues that are not energetically liked to KCNE1 are colored blue. Putative contacts (atom distances ≤ 3 Å) of KCNQ1 and KCNE1 atoms were computed and are indicated by thin lines. The number of atom contacts between KCNQ1 and KCNE1 residues was plotted vs. the energetic perturbance values described by Shamgar [23] (right panel). The methionine side chain of KCNQ1-M238 points into the center of the voltage sensor domain S1-S4 and may stabilize it. M238 has only weak contact with KCNE1, but can strongly disturb complex energetics upon mutation. Thus, effects by mutation of this residue cannot be simply explained by disturbance of direct interactions with KCNE1, but instead suggest indirect coupling. c, The KCNQ1/KCNE1 model was scanned for transmembrane helices and inserted into a Pch/Pea/Pse (1:1:1) membrane based on the transmembrane scan results. A 0.6 ns MD simulation was run to equilibrate the system. The voltage sensor domain is shown in red (left picture) and the KCNQ1 residue A226 (green) is shown in space fill. The phosphates of the phospholipids are shown in yellow and space fill and the position of the membrane is further indicated by a dashed orange line. A close-up view is shown to the right. Water molecules in proximity to A226 are shown in space fill (middle). As residue A226 is located in a water-filled crevice open to the outer environment, this residue can be state-dependently chemically modified, as reported experimentally [21, 22]. d, The average KCNQ1/KCNE1 structure was cut at the level of the residues F339/F340 and the central cavity. The KCNQ1 backbone and KCNE1 are colored blue and yellow, respectively. While the side chains of F340 point to the central cavity in a standard KCNQ1 homology model, they are repositioned during the MD simulation in the presence of KCNE1 to point away from the central cavity (The pdb-file can be downloaded from our web-page under: http://www.ruhr-uni-bochum.de/bc1/kation/download/Q1E1-nach_50_ns_sim_average_a.pdb).

In the case of interaction of the π-electron system of F339 with the hydroxyl group of T58, a hydrogen bond may be formed in one KCNQ1-KCNE1 system. In both systems, the position of the aromatic side chain of KCNQ1-F339 is very stable, suggesting strong interactions with KCNE1-T58.

- The hydroxyl group of KCNQ1-S338 is expected to make direct contact/hydrogen bonding with residue T58 in KCNE1 in agreement with the expectations of a hydrogen bond from the experimental data. As can be seen in Fig. 3b,c, both residues form hydrogen bonds during the main course of the MD simulation.

- KCNQ1-F270 and KCNQ1-F340 serve to position S338 and F339 enabling the hydrogen bonding and volume effects consistent with the important functions of these residues suggested from the energetic

coupling analyses (Fig. 2).

- KCNE1-F57 π-stacks with KCNQ1-F270, a strong interaction that explains why the F270A mutation causes a strong energetic perturbation.

Our KCNQ1/KCNE1 model is consistent with previous experimental findings: An interaction of the KCNE1 residues 55 and 56 with C331 in KCNQ1 that has been demonstrated by crosslinking experiments would theoretically be possible in our model with minor repositioning of KCNE1 [36]. Potential interactions of KCNQ1 residues S338, F339, and F340 with KCNE1 residues T58 and G59 have previously been proposed and are consistent with our model [18, 19, 28]. Lerche et al. showed that KCNE1 does not line the central cavity, which is in agreement with our model and our experimental data showing that binding of a specific inhibitor to the central cavity is not disrupted by a KCNE1 mutation along the transmembrane domain [16].

Our dynamic molecular model provides explanations for various effects of KCNE1 on KCNQ1 channel pharmacology. For instance, a benzodiazepine agonist of KCNQ1 has no effect when KCNE1 is present [37]. Our model now demonstrates that the binding site for this agonist in KCNQ1 overlaps with the KCNQ1-KCNE1 interaction site and is thus blocked by binding of KCNE1 to KCNQ1. Moreover, the model shows that interaction of KCNE1 with the central S6 α-helix of KCNQ1 would reposition the key residues for the block by benzodiazepine L7 and chromanol 293B, F339 and F340, to enable the higher affinity of binding observed for KCNQ1/KCNE1 channels compared to KCNQ1 alone (Fig. 4d) [16, 30]. Residues crucial for the activation of KCNQ1/KCNE1 channels by stilbenes and fenamates can be expected to be accessible from our model, which would enable the pharmacological action of the compounds [38].

For our model, we used a stoichiometry of four KCNQ1 subunits to two KCNE1 subunits, resulting in a very stable model. However, other stoichiometries of KCNQ1 to KCNE1 subunits are theoretically possible and could be simulated by addition or deletion of KCNE1 peptides [12-14].

The combination of experimental data and the molecular dynamics-derived 3D-model suggests that the KCNE1 transmembrane domain binds to a cleft between the pore module and the voltage sensor module of KCNQ1. This specific KCNQ1 conformation represents a closed state that is stabilized by helix-helix interactions, hydrophobic interactions, van-der-Waals interactions,

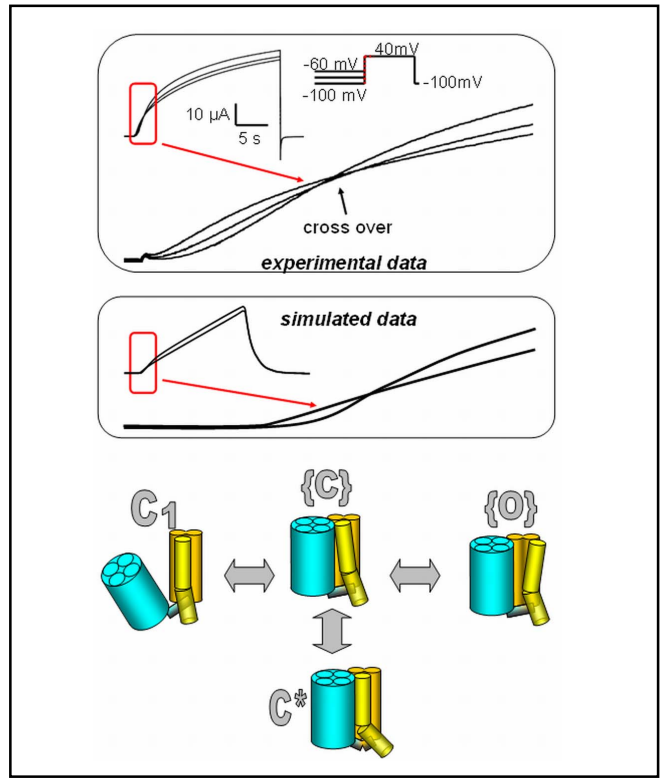

Fig. 5. Asignment of the 3D model of the KCNQ1/KCNE1 channel to kinetic states. KCNQ1/KCNE1 channels were expressed in oocytes and currents were elicited by 40 mV pulses after applying prepulses. Currents show a prominent cross over phenomenon after about 1.75 s. The kinetic behavior of KCNQ1/KCNE1 channels can be described by a modified KCNQ1 gating model [9, 10] incorporating an additional closed inactivated state C* [43]. This kinetic model is shown below. Prepulsing to -60mV or -100mV results in the characteristic cross-over in the simulated current traces. Additional information on the kinetic model is given in supplementary material (http://www.ruhr-uni-bochum.de/bc1/kation/download/Strutz-See-bohm_et_al_Cell_Physiol_Biochem_supplementary_material.doc).

π-stacking of aromatic residues, and a hydrogen bond between KCNQ1-S338 and KCNE1-T58. This stabilization of the closed channel state of KCNQ1 by interaction with KCNE1 may represent the molecular basis of right-shifted G/V curves and slowed activation. When the KCNQ1/KCNE1 channels activate/open, KCNE1 may slide from the pre-open position described here to a different relative position in the channel complex called "activation cleft" to increase current amplitudes [23-31]. Crosslinking studies of cysteines introduced in the S1 domain of KCNQ1 with engineered cysteines in KCNE1 suggested that KCNE1 is involved in molecular movements during channel gating [20]. Moreover, state-

dependent modification by MTS of a cysteine engineered into the S4 voltage sensor domain of KCNQ1 (A226C) was slowed 13-fold by KCNE1, suggesting that KCNE1 slows the transition of the voltage sensor to the open state [22]. However, a second study showed uncoupling of state-dependent MTS modification from pulse durations in a set of KCNQ1 cysteine mutants, suggesting that the voltage sensor can quickly adopt an open conformation, and slow activation cannot be a direct result from slowed voltage sensor transition to the open state. Thus, it is likely that our dynamically stable KCNQ1/KCNE1 model provides only a snapshot of one state. However, this modeled state may represent one of the frequently occupied stable states. In our model the KCNE1 peptide destabilizes the S4-S5 linker α-helical structure and the interacting lower S6 α-helical structure. The destabilization of S4-S5 and the lower S6 may cause an uncoupling of the voltage sensor movement from the opening of the bundle crossing. The result would be an uncoupling of the voltage sensor movement from channel activation. Such an uncoupling would lead to slowed activation kinetics, which are a hallmark of native cardiac KCNQ1/KCNE1 channels.

The slowing of the activation and deactivation kinetics observed in KCNQ1/KCNE1 channels compared to homomeric KCNQ1 possibly reflects an increased energy barrier between different gating states. Furthermore, KCNQ1 shows an open state inactivation/flickery block not present in KCNQ1/KCNE1 channels under standard conditions [39, 40]. Thus, this open inactivated state does not have to be accounted for in a KCNQ1/KCNE1 kinetic model. However, there is an additional peculiarity present in KCNQ1/KCNE1 gating. When preceded by a negative prepulse, voltage-dependent channel activation is initially slow, but later currents become larger compared to currents elicited without using a prepulse [41]. This crossover effect is illustrated in Fig. 5. This phenomenon cannot be explained by a simple linear gating scheme [42] such as:

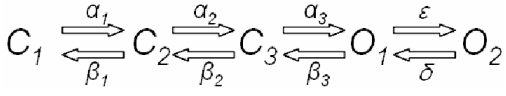

However, the introduction of a closed inactivated state C* as depicted below:

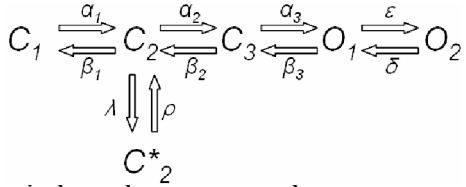

recapitulates the crossover phenomenon, as long as the state is made absorbing enough (see Fig. 5). With a negative prepulse, channels reside mostly in C_1 and "pass over" the inactivated state C^*_2, leading to full current activation. With a less negative prepulse, the activation kinetics are initially faster because channels start from states in which part of the voltage sensors are already activated. However, the current that can be activated is actually smaller because the inactivated state is substantially populated.

The state presented by our dynamic 3D KCNQ1/KCNE1 model could represent the structural correlate of the closed inactivated state C*, as it fulfills several prerequisites. First, the modeled state is based on a voltage sensor domain in the activated ("up") position representing an open or open inactivated state. However, by destabilization of the ordered structure of the opened bundle, crossing the ion passage is compromised and this state can be expected to be non-conductive. Further, the modeled state seems to be relatively stable, as it would be expected for C*. Negative prepulses may shift the equilibrium of channels towards channels with voltage sensors in the deactivated ("down") position, which can be expected to disrupt interaction between KCNE1, the pore and voltage sensor domains. As a consequence of reduced local interaction with KCNQ1, KCNE1 may be relieved from its relative C* position to adopt a different conformation in the channel complex. Such relative flexibility of KCNE1 within the channel complex is consistent with recent experimental findings [21]. Clearly, further data is required to verify the hypothesis of a preopen closed state.

Concluding, we present a dynamic 3-D structural model of the KCNQ1-KCNE1-interaction based on a large set of new and previously published data. We suggest a model that positions KCNE1 in close proximity to transmembrane domains S4, S5, and S6 of KCNQ1 and allows modulation of the pore module S5/S6, possibly stabilizing a pre-open closed state. This model will be useful in studying the structural and dynamic effects of diverse LQTS mutant channels and may prove helpful in determining the specific molecular pharmacology of cardiac I_{Ks} channels.

Acknowledgements

We thank Gildas Loussouarn for comments on the manuscript. This work was supported by Telethon Italy (grant GGP04018) and the Italian Institute of Technology ("progetto SEED"). The support of GS by a DFG-grant

SE1077/3-1 and SFB 642 (also to K. G. and R. S.) is gratefully acknowledged. S. W. is funded by a CAS Young International Scientist Fellowship. We thank the RRZ Köln for additional computing time. The model-pdb-file and supplementary material can be downloaded from our web-page under: http://www.ruhr-uni-bochum.de/bc1/kation/download/Q1E1-nach_50_ns_sim_average_a.pdb and http://www.ruhr-uni-bochum.de/bc1/kation/download/Strutz-Seebohm_et_al_Cell_Physiol_Biochem_supplementary_material.doc , respectively.

References

1 Barhanin J, Lesage F, Guillemare E, Fink M, Lazdunski M, Romey G: K(V)LQT1 and lsK (minK) proteins associate to form the I(Ks) cardiac potassium current. Nature 1996;384:78-80.

2 Sanguinetti MC, Curran ME, Zou A, Shen J, Spector PS, Atkinson DL, Keating MT: Coassembly of K(V)LQT1 and minK (IsK) proteins to form cardiac I(Ks) potassium channel. Nature 1996;384:80-83.

3 Abbott GW, Sesti F, Splawski I, Buck ME, Lehmann MH, Timothy KW, Keating MT, Goldstein SA: MiRP1 forms IKr potassium channels with HERG and is associated with cardiac arrhythmia. Cell 1999;97:175-187.

4 Decher N, Bundis F, Vajna R, Steinmeyer K: KCNE2 modulates current amplitudes and activation kinetics of HCN4: influence of KCNE family members on HCN4 currents. Pflugers Arch 2003;446:633-640.

5 Grunnet M, Rasmussen HB, Hay-Schmidt A, Rosenstierne M, Klaerke DA, Olesen SP, Jespersen T: KCNE4 is an inhibitory subunit to Kv1.1 and Kv1.3 potassium channels. Biophys J 2003;85:1525-1537.

6 McCrossan ZA, Lewis A, Panaghie G, Jordan PN, Christini DJ, Lerner DJ, Abbott GW: MinK-related peptide 2 modulates Kv2.1 and Kv3.1 potassium channels in mammalian brain. J Neurosci 2003;23:8077-8091.

7 Deschenes I, Tomaselli GF: Modulation of Kv4.3 current by accessory subunits. FEBS Lett 2002;528:183-188.

8 Abbott GW, Goldstein SA, Sesti F: Do all voltage-gated potassium channels use MiRPs? Circ Res 2001;88:981-983.

9 Pusch M, Magrassi R, Wollnik B, Conti F: Activation and inactivation of homomeric KvLQT1 potassium channels. Biophys J 1998;75:785-792.

10 Tristani-Firouzi M, Sanguinetti MC: Voltage-dependent inactivation of the human K^+ channel KvLQT1 is eliminated by association with minimal K^+ channel (minK) subunits. J Physiol 1998;510:37-45.

11 Seebohm G, Scherer CR, Busch AE, Lerche C: Identification of specific pore residues mediating KCNQ1 inactivation. A novel mechanism for long QT syndrome. J Biol Chem 2001;276:13600-13605.

12 Wang W, Xia J, Kass RS: MinK-KvLQT1 fusion proteins, evidence for multiple stoichiometries of the assembled IsK channel. J Biol Chem 1998;273:34069-34074.

13 Chen H, Kim LA, Rajan S, Xu S, Goldstein SA: Charybdotoxin binding in the I(Ks) pore demonstrates two MinK subunits in each channel complex. Neuron 2003;40:15-23.

14 Morin TJ, Kobertz WR: Counting membrane-embedded KCNE beta-subunits in functioning K^+ channel complexes. Proc Natl Acad Sci USA 2008;105:1478-1482.

15 Chen H, Sesti F, Goldstein SA: Pore- and state-dependent cadmium block of I(Ks) channels formed with MinK-55C and wild-type KCNQ1 subunits. Biophys J 2003;4:3679-3689.

16 Lerche C, Seebohm G, Wagner CI, Scherer CR, Dehmelt L, Abitbol I, Gerlach U, Brendel J, Attali B, Busch AE: Molecular impact of MinK on the enantiospecific block of I(Ks) by chromanols. Br J Pharmacol 2000;131:1503-1506.

17 Melman YF, Um SY, Krumerman A, Kagan A, McDonald TV: KCNE1 binds to the KCNQ1 pore to regulate potassium channel activity. Neuron 2004;42:927-937.

18 Panaghie G, Tai KK, Abbott GW: Interaction of KCNE subunits with the KCNQ1 K^+ channel pore. J Physiol 2005;570:455-467.

19 Tai KK, Goldstein SA: The conduction pore of a cardiac potassium channel. Nature 1998;391:605-608.

20 Xu X, Jiang M, Hsu KL, Zhang M, Tseng GN: KCNQ1 and KCNE1 in the IKs channel complex make state-dependent contacts in their extracellular domains. J Gen Physiol 2008;131:589-603.

21 Nakajo K, Kubo Y: KCNE1 and KCNE3 stabilize and/or slow voltage sensing S4 segment of KCNQ1 channel. J Gen Physiol 2007;130:269-281.

22 Rocheleau JM, Kobertz WR: KCNE peptides differently affect voltage sensor equilibrium and equilibration rates in KCNQ1 K^+ channels. J Gen Physiol 2008;131:59-68.

23 Shamgar L, Haitin Y, Yisharel I, Malka E, Schottelndreier H, Peretz A, Paas Y, Attali B: KCNE1 constrains the voltage sensor of Kv7.1 K^+ channels. PLoS One 2008;3:e1943.

24 Aggeli A, Bannister ML, Bell M, Boden N, Findlay JB, Hunter M, Knowles PF, Yang JC: Conformation and ion-channeling activity of a 27-residue peptide modeled on the single-transmembrane segment of the IsK (minK) protein. Biochemistry 1998;37:8121-8131.

25 Tian C, Vanoye CG, Kang C, Welch RC, Kim HJ, George AL, Sanders CR: Preparation, functional characterization, and NMR studies of human KCNE1, a voltage-gated potassium channel accessory subunit associated with deafness and long QT syndrome. Biochemistry 2007;46:11459-11472.

26 Vakser IA, Matar OG, Lam CF: A systematic study of low-resolution recognition in protein-protein complexes. Proc Natl Acad Sci USA,1999;96:8477-8482.
27 Van Der Spoel D, Lindahl E, Hess B, Groenhof G, Mark AE, Berendsen HJ: GROMACS: fast, flexible, and free. J Comput Chem 2005;26:1701-1718.
28 Attali B, Guillemare E, Lesage F, Honore E, Romey G, Lazdunski M, Barhanin J: The protein IsK is a dual activator of K^+ and Cl^- channels. Nature 1993;365:850-852.
29 Kang C, Tian C, Sönnichsen FD, Smith JA, Meiler J, George AL, Vanoye CG, Kim HJ, Sanders CR: Structure of KCNE1 and implications for how it modulates the KCNQ1 potassium channel. Biochemistry 2008;47:7999-8006.
30 Seebohm G, Chen J, Strutz N, Culberson C, Lerche C, Sanguinetti MC: Molecular determinants of KCNQ1 channel block by a benzodiazepine. Mol Pharmacol 2003;64:70-77.
31 Horovitz A: Double-mutant cycles: a powerful tool for analyzing protein structure and function. Fold Des 1996;1:R121-126.
32 Melman YF, Krumerman A, McDonald TV: A single transmembrane site in the KCNE-encoded proteins controls the specificity of KvLQT1 channel gating. J Biol Chem 2002;277:25187-25194.
33 Long SB, Campbell EB, Mackinnon R: Crystal structure of a mammalian voltage-dependent Shaker family K^+ channel. Science 2005;309:897-903.
34 Chen X, Wang Q, Ni F, Ma J: Structure of the full-length Shaker potassium channel Kv1.2 by normal-mode-based X-ray crystallographic refinement. Proc Natl Acad Sci USA 2010;107:11352-11357.
35 Smith JA, Vanoye CG, George AL, Meiler J, Sanders CR: Structural models for the KCNQ1 voltage-gated potassium channel. Biochemistry 2007;46:14141-14152.
36 Tapper AR, George AL: Location and orientation of minK within the I(Ks) potassium channel complex. J Biol Chem 2001;276:38249-38254.
37 Seebohm G, Pusch M, Chen J, Sanguinetti MC: Pharmacological activation of normal and arrhythmia-associated mutant KCNQ1 potassium channels. Circ Res 2003;93:941-947.
38 Abitbol I, Peretz A, Lerche C, Busch AE, Attali B: Stilbenes and fenamates rescue the loss of I(KS) channel function induced by an LQT5 mutation and other IsK mutants. EMBO J 1999;18:4137-4148.
39 Seebohm G, Sanguinetti MC, Pusch M: Tight coupling of rubidium conductance and inactivation in human KCNQ1 potassium channels. J Physiol 2003;552:369-378.
40 Pusch M, Bertorello L, Conti F: Gating and flickery block differentially affected by rubidium in homomeric KCNQ1 and heteromeric KCNQ1/KCNE1 potassium channels. Biophys J 2000;78:211-226.
41 Cole KS, Moore JW: Potassium ion current in the squid giant axon. Biophys J 1960;1:161-202.
42 Tzounopoulos T, Maylie J, Adelman JP: Gating of I(sK) channels expressed in Xenopus oocytes. Biophys J 1998;74:2299-2305.
43 Pusch M: Analysis of Electrophysiological Data; in Clare JJ, Trezise DJ (eds): Expression and Analysis of Recombinant Ion Channels: From Structural Studies to Pharmacological Screening. Wiley, Weinheim, 2006.